

1 Collision energy dependence of C_5 and C_6 of 2 net-proton distributions at RHIC-STAR

Ashish Pandav for the STAR collaboration^{*†}

School of Physical Sciences, National Institute of Science Education and Research, HBNI,

Jatni-752050, INDIA

E-mail: apandav10@gmail.com

Cumulants of net-baryon distributions are predicted to be sensitive observables in the study of the QCD phase diagram. The cumulant ratios are related to the thermodynamic susceptibilities which can be obtained from QCD based models, HRG, and lattice QCD calculations. QCD thermodynamics with a cross-over predicts negative sign of fifth- and sixth-order baryon number fluctuations. Furthermore, higher order proton factorial cumulants are also suggested to carry signals of the first-order phase transition between hadronic phase and the QGP, where the proton multiplicity distributions could develop a two-component structure.

We report the measurements of fifth- and sixth-order cumulants of net-proton distributions in Au+Au collisions from $\sqrt{s_{NN}} = 7.7 - 200$ GeV, recorded by the STAR detector in the phase I of Beam Energy Scan (BES-I) program at RHIC. In addition, factorial cumulants of proton distributions for Au+Au collisions at $\sqrt{s_{NN}} = 7.7$ GeV are also presented. While C_5/C_1 of net-proton distributions in 0-40% centrality shows a weak collision energy dependence and fluctuates around zero, the C_6/C_2 values are increasingly negative with decreasing energy for the same centrality. Results of the two ratios for peripheral 70-80% collisions are positive at all energies. Within large uncertainties, the proton factorial cumulant κ_5 shows agreement with expectation from first-order transition inspired two-component model calculations while κ_6 remains 1.8σ away from the predictions for 0-5% centrality.

CPOD2021 - the International conference on Critical Point and Onset of Deconfinement

15 - 19 March 2021

Online via Zoom

^{*}Speaker.

[†]

3 1. Introduction

4 Strong interactions, one of the four fundamental interactions in nature, are governed by theory
5 of Quantum Chromodynamics (QCD). The phase diagram of strongly interacting matter, known
6 as the QCD phase diagram, represented on the plane of temperature (T) and baryonic chemical
7 potential (μ_B) is largely conjectured. It has at least two distinct phases: the Quark-Gluon-Plasma
8 (QGP) [1] and the hadronic phase [2, 3]. While the quarks and gluons are deconfined in the QGP,
9 they are confined in the hadronic phase. QCD calculations on lattice has proven the nature of phase
10 transition between the two phases at vanishing μ_B to be a crossover [4]. Lattice QCD calculations
11 at finite μ_B suffer from the notorious sign-problem. However, QCD-based model calculations at
12 finite μ_B suggest the cross-over changes to be a first-order phase transition accompanied by the
13 QCD critical point [5, 6].

14 So far there has been no direct experimental evidence of the cross-over and first order phase
15 transition. Study of the QCD phase diagram is facilitated by experimental measurements of cumu-
16 lants of event-by-event net-particle distributions as proxy for conserved quantum numbers (B,Q,S)
17 in heavy-ion nuclear collisions [7, 8, 9, 10, 11, 12]. The ratios of cumulants are directly related
18 to thermodynamic susceptibilities calculable in lattice-QCD, QCD-based model, and hadron res-
19 onance gas (HRG) model [13, 14, 15]. Recently, lattice QCD calculations with cross-over as the
20 nature of phase transition have been extended to finite μ_B ($\mu_B \leq 160$ MeV) using taylor series
21 expansion about vanishing μ_B , thus avoiding the sign-problem. It predicts negative sign for ratio
22 of fifth-to-first (χ_5^B/χ_1^B) and sixth-to-second (χ_6^B/χ_2^B) order baryon number susceptibilities [16]. It
23 also advocates increasingly negative values of the two susceptibility ratios with increasing μ_B . Cal-
24 culations from functional renormalisation group (FRG) model also predict the same sign and μ_B
25 dependence for the fifth- and sixth-order net-baryon susceptibility ratios for a wide μ_B range of 20 -
26 420 MeV corresponding to STAR Au+Au collision energies $\sqrt{s_{NN}} = 200 - 7.7$ GeV [17]. Further-
27 more, measurements of proton factorial cumulants have been suggested as sensitive observables to
28 probe first-order phase transition. Near the vicinity of the first-order phase transition, a bimodal or
29 two-component distribution is expected for proton multiplicity which results in a unique trait of
30 factorial cumulants: their magnitude increases with order and flips sign [18, 19].

31 Recent STAR results on fourth-order net-proton cumulant ratio C_4/C_2 were found to exhibit
32 non-monotonic collision energy dependence which is qualitatively consistent with a QCD-based
33 model calculation that includes a critical point [11]. The study presented in this proceedings ex-
34 tends the net-proton and proton fluctuation measurements to fifth- and sixth-order to study the
35 nature of phase transition by examining the sign-change of the measurements. Collision energy
36 dependence of net-proton C_5/C_1 and C_6/C_2 for central 0-40% and peripheral 70-80% Au+Au col-
37 lisions from $\sqrt{s_{NN}} = 7.7 - 200$ GeV is presented where the percentage denotes the fraction of the
38 total cross-section. Proton factorial cumulants as a function of centrality in $\sqrt{s_{NN}} = 7.7$ GeV gold
39 nucleus collisions are reported. Comparisons of measurements with various theoretical predictions
40 are also shown.

41 2. Observables

42 The observables for our study are the nth-order cumulants (C_n) and factorial cumulants (κ_n) of

43 net-proton and proton distributions, respectively. Cumulants can be expressed purely with factorial
 44 cumulants and vice versa. The cumulants of a distribution quantify the traits of the distribution.
 45 For example, the first and second order cumulant are the well known mean and variance of a
 46 distribution. Similarly, the third and fourth order cumulants reflect its skewness and kurtosis. This
 47 work extends the order of cumulants to fifth and sixth-order, which are defined as follows:

$$C_5 = \langle(\delta N)^5\rangle - 5\langle(\delta N)^3\rangle\langle(\delta N)^2\rangle, \quad (2.1)$$

$$C_6 = \langle(\delta N)^6\rangle - 15\langle(\delta N)^4\rangle\langle(\delta N)^2\rangle - 10\langle(\delta N)^3\rangle^2 + 30\langle(\delta N)^2\rangle^3, \quad (2.2)$$

48 Here, N is the observable of our interest, for example net-proton number and $\delta N = N - \langle N \rangle$ where
 49 $\langle N \rangle$ is the average of the N across all events. The fifth and sixth order factorial cumulants for a
 50 variate can be expressed in terms of its cumulants as follows:

$$\kappa_5 = 24C_1 - 50C_2 + 35C_3 - 10C_4 + C_5, \quad (2.3)$$

$$\kappa_6 = -120C_1 + 274C_2 - 225C_3 + 85C_4 - 15C_5 + C_6, \quad (2.4)$$

51 3. Analysis Details

52 Data of Au+Au collisions at nine energies: $\sqrt{s_{NN}} = 7.7, 11.5, 14.5, 19.6, 27, 39, 54.4, 62.4$
 53 and 200 GeV were analysed as part of the first phase of beam energy scan (BES-I) program at
 54 Relativistic Heavy-ion Collider (RHIC) facility. The number of minimum bias events range from 3
 55 millions at $\sqrt{s_{NN}} = 7.7$ GeV to about 900 millions at $\sqrt{s_{NN}} = 200$ GeV. The detectors used for (anti-
 56)proton identification are the Time-Projection-Chamber (TPC) and Time-of-Flight (TOF) [20]. The
 57 charged particle multiplicity in the psuedo-rapidity (η) range $|\eta| < 1$ are used to define centrality.
 58 As the fluctuations of net-protons are the observables of interest, protons and anti-protons are ex-
 59 cluded from centrality definition to avoid self-correlation effects. The (anti-)protons at mid-rapidity
 60 ($|y| < 0.5$) within the transverse momentum (p_T) coverage of $0.4 < p_T < 2.0$ GeV/ c are used for
 61 measurements. In the p_T range of $0.4 < p_T < 0.8$ GeV/ c , only the TPC is used to select (anti-
 62)protons whereas one requires both TPC and TOF for (anti-)proton identification in the higher mo-
 63 mentum region, $0.8 < p_T < 2.0$ GeV/ c . To suppress the background to the cumulant measurements
 64 arising due to initial system volume fluctuations, a method called Centrality-Bin-Width-Correction
 65 (CBWC) was applied [21]. To correct the cumulants for finite detector efficiency, an analytical
 66 correction was performed where the detector response was assumed to follow binomial distribu-
 67 tion [22, 23, 24]. For estimation of statistical uncertainties, bootstrap method was used [25, 26, 27].
 68 Systematic uncertainties on the measurements were estimated varying tracking efficiency, track se-
 69 lection and particle identification criteria.

70 4. Results

71 4.1 Energy dependence of net-proton C_5/C_1 and C_6/C_2

72 The cumulants ratios C_5/C_1 and C_6/C_2 of net-proton distributions in Au+Au collisions from
 73 $\sqrt{s_{NN}} = 7.7 - 200$ GeV for collision centralities 0-40% and 70-80% centralities are presented in
 74 panel (1) and (2) of Fig. 1, respectively. The 0-40% central C_5/C_1 measurements show weak

75 collision centrality dependence and fluctuate around zero in the whole collision energy range at
 76 a level of $\leq 2\sigma_{tot}$, where σ_{tot} is the total uncertainties on the data obtained adding statistical and
 77 systematic uncertainties in quadrature. The peripheral 70-80% C_5/C_1 ratios at all energies are
 78 positive and close to poisson baseline of unity. The C_6/C_2 for 0-40% centrality shows increasingly
 79 negative values with decreasing energy. In contrast, the HRG canonical ensemble calculations with
 80 no phase transition incorporated are mostly positive and become negative at very low energies.
 81 Except at 7.7 GeV, where the transport model UrQMD [29] calculations with impact parameter
 82 $b < 3$ fm are positive for both net-proton C_5/C_1 and C_6/C_2 , the calculations have too large statistical
 83 uncertainties to show a definite sign. The peripheral 70-80% C_6/C_2 data are found to be positive at
 all energies.

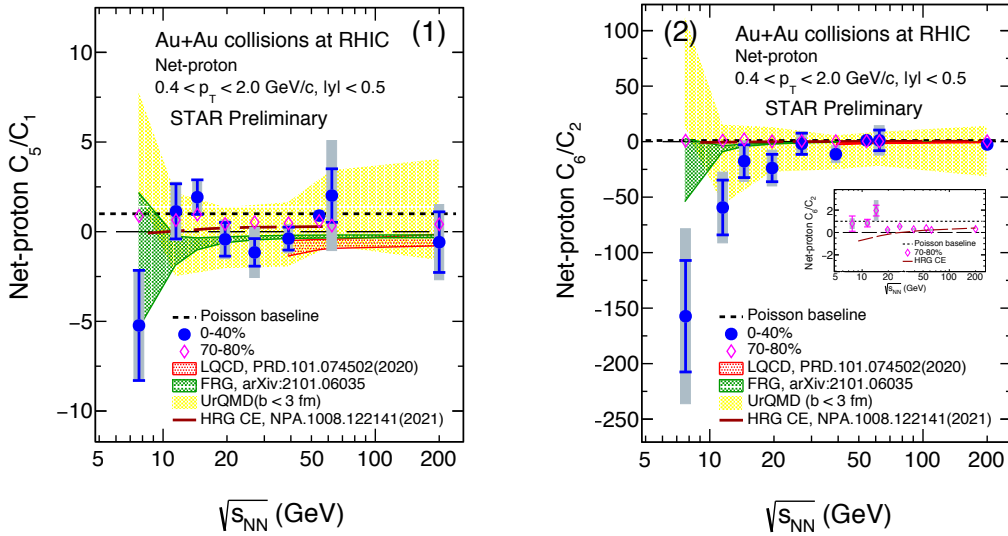


Figure 1: C_5/C_1 (1) and C_6/C_2 (2) of net-proton distributions in Au+Au collisions from $\sqrt{s_{NN}} = 7.7 - 200$ GeV for central (0-40%, solid blue circles) and peripheral collisions (70-80%, open magenta diamond). The bars and golden shaded bands on the data points represent the statistical and systematic uncertainties, respectively. Calculations from lattice QCD (39 – 200 GeV) [16], FRG (7.7 – 200 GeV) [17], UrQMD model and HRG model with canonical ensemble [28] are shown in red, green, yellow bands and brown dashed line, respectively. The dotted line at unity represents the poisson baseline. The inset in panel (2) contains peripheral 70-80% C_6/C_2 data.

84

85 4.2 Proton factorial cumulants κ_5 and κ_6 in Au+Au collisions at $\sqrt{s_{NN}} = 7.7$ GeV

86 Fifth and sixth-order factorial cumulants of proton multiplicity distributions as a function of
 87 collision-centrality (given by average number of participant nucleons, $\langle N_{part} \rangle$) is shown in panel
 88 (1) and (2) of Fig. 2, respectively. The κ_5 measurements are increasingly negative as a function of
 89 $\langle N_{part} \rangle$ while the κ_6 shows little collision-centrality dependence. Calculation from two-component
 90 model, which assumes a two-component distribution for proton multiplicity with the measured
 91 factorial cumulants up to fourth-order as inputs in its construction [12], predicts negative κ_5 and
 92 positive κ_6 for 0-5% centrality. While the result of κ_5 for 0-5% centrality is consistent with the
 93 two-component model expectation within uncertainties, the result of κ_6 remains $1.8 \sigma_{tot}$ away

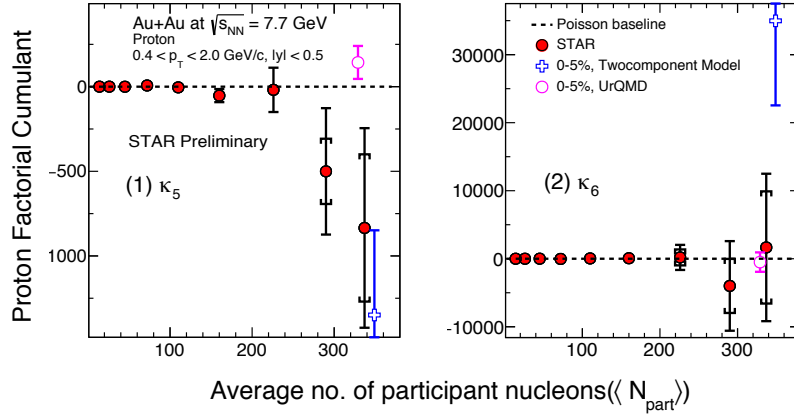


Figure 2: κ_5 (1) and κ_6 (2) of proton distributions in Au+Au collisions at $\sqrt{s_{NN}} = 7.7$ GeV as a function of average number of participant nucleons. The STAR measurements are shown in red solid markers. The bars and caps on the data points represent the statistical and systematic uncertainties, respectively. The poisson baseline is shown as the dotted line. The two-component model and UrQMD model expectations for the 0-5% centrality are shown as blue cross and open magenta markers, respectively.

94 from the prediction for the same centrality and is consistent with the poisson baseline albeit with
 95 large uncertainties. The UrQMD calculations for both the order of factorial cumulants are close to
 96 poisson baseline of zero.

97 5. Summary

98 In summary, we presented measurements on collision energy dependence of net-proton cu-
 99 mulant ratios C_5/C_1 and C_6/C_2 for 0-40% and 70-80% collision centrality for a wide range of
 100 collision energies from $\sqrt{s_{NN}} = 7.7$ to 200 GeV, which corresponds to μ_B range of 420 - 20 MeV,
 101 respectively. The net-proton C_5/C_1 for 0-40% centrality shows weak collision energy dependence.
 102 The net-proton C_6/C_2 for the same centrality shows increasingly negative values with decreasing
 103 collision energy at a level of $\leq 2\sigma_{tot}$. In contrast, the peripheral 70-80% data for both ratios are
 104 found to be positive at all energies. It is noteworthy to mention here that lattice-QCD and FRG
 105 calculations predict negative fifth and sixth-order baryon-number susceptibility ratios which be-
 106 come more negative with increasing μ_B , or in other words, decreasing collision energy. Here, when
 107 comparing the experimental data to theoretical calculations from lattice-QCD and FRG model one
 108 should keep in mind that in contrast to the latter which predict on fluctuations of conserved quan-
 109 tity net-baryon, the experimental measurements are made instead for net-protons. Also, as opposed
 110 to the theoretical calculation, the experimental measurements are done within a finite phase-space
 111 acceptance determined by experimental limitations of the detectors. These caveats should be ac-
 112 counted in future to facilitate a quantitative comparison between the theory and data. Furthermore,
 113 comparison of fifth and sixth order proton factorial cumulants with expectation from a first-order
 114 transition inspired two-component model for 0-5% centrality shows agreement within uncertainties
 115 for κ_5 , while the result of κ_6 remains 1.8σ away from the model prediction. The current measure-

116 ments suffer from large uncertainties, and thus precision measurements in BES-II will be necessary
117 in order to confirm the reported dependence of fifth- and sixth-order fluctuations.

118 **References**

- 119 [1] E. V. Shuryak, Phys. Rept. **61**, 71-158 (1980)
120 [2] L. McLerran and R. D. Pisarski, Nucl. Phys. A **796**, 83-100 (2007)
121 [3] P. Braun-Munzinger and J. Wambach, Rev. Mod. Phys. **81**, 1031-1050 (2009)
122 [4] Y. Aoki, G. Endrodi, Z. Fodor, S. D. Katz and K. K. Szabo, Nature **443**, 675-678 (2006)
123 [5] S. Ejiri, Phys. Rev. D **78**, 074507 (2008)
124 [6] E. S. Bowman and J. I. Kapusta, Phys. Rev. C **79**, 015202 (2009)
125 [7] L. Adamczyk *et al.* [STAR Collaboration], Phys. Rev. Lett. **113**, 092301 (2014).
126 [8] L. Adamczyk *et al.* [STAR Collaboration], arXiv:1709.00773 [nucl-ex].
127 [9] M. M. Aggarwal *et al.* [STAR Collaboration], Phys. Rev. Lett. **105**, 022302 (2010)
128 [10] L. Adamczyk *et al.* [STAR Collaboration], Phys. Rev. Lett. **112**, 032302 (2014)
129 [11] J. Adam *et al.* [STAR Collaboration], Phys. Rev. Lett. **126**, 092301 (2021)
130 [12] M. Abdallah *et al.* [STAR], Phys. Rev. C **104**, no.2, 024902 (2021)
131 [13] R. V. Gavai and S. Gupta, Phys. Lett. B **696**, 459 (2011)
132 [14] S. Gupta, X. Luo, B. Mohanty, H. G. Ritter and N. Xu, Science **332**, 1525 (2011)
133 [15] F. Karsch and K. Redlich, Phys. Lett. B **695**, 136-142 (2011)
134 [16] A. Bazavov, D. Bollweg, H. T. Ding, P. Enns, J. Goswami, P. Hegde, O. Kaczmarek, F. Karsch,
135 R. Larsen and S. Mukherjee, *et al.* Phys. Rev. D **101**, no.7, 074502 (2020)
136 [17] W. j. Fu, X. Luo, J. M. Pawłowski, F. Rennecke, R. Wen and S. Yin, [arXiv:2101.06035 [hep-ph]].
137 [18] A. Bzdak, V. Koch, Phys. Rev. C (R) **100**, 014901 (2019)
138 [19] A. Bzdak, V. Koch, D. Oliinychenko and J. Steinheimer, Phys. Rev. C **98**, no.5, 054901 (2018)
139 [20] K. H. Ackermann *et al.* [STAR], Nucl. Instrum. Meth. A **499**, 624-632 (2003)
140 [21] X. Luo, J. Xu, B. Mohanty and N. Xu, J. Phys. G **40**, 105104 (2013)
141 [22] X. Luo, Phys. Rev. C **91**, no.3, 034907 (2015) [erratum: Phys. Rev. C **94**, no.5, 059901 (2016)]
142 [23] T. Nonaka, M. Kitazawa and S. Esumi, Phys. Rev. C **95**, no. 6, 064912 (2017)
143 [24] X. Luo and T. Nonaka, Phys. Rev. C **99**, no.4, 044917 (2019)
144 [25] B. Efron, The Annals of Statistics **7** p1-26(1979)
145 [26] X. Luo, J. Phys. G **39**, 025008 (2012)
146 [27] A. Pandav, D. Mallick and B. Mohanty, Nucl. Phys. A **991**, 121608 (2019)
147 [28] P. Braun-Munzinger, B. Friman, K. Redlich, A. Rustamov and J. Stachel, Nucl. Phys. A **1008**, 122141
148 (2021)
149 [29] M. Bleicher, E. Zabrodin, C. Spieles, S. A. Bass, C. Ernst, S. Soff, L. Bravina, M. Belkacem,
150 H. Weber and H. Stoecker, *et al.* J. Phys. G **25**, 1859-1896 (1999)